THE ASTROPHYSICAL JOURNAL, 437:683–696, 1994 December 20

NEAR-INFRARED ABSORPTION SPECTROSCOPY OF INTERSTELLAR HYDROCARBON GRAINS

Y. J. PENDLETON,[1] S. A. SANDFORD,[2,3] L. J. ALLAMANDOLA,[2,3]
A. G. G. M. TIELENS,[1] AND K. SELLGREN[3,4,5]
Received 1994 April 25; accepted 1994 June 23

ABSTRACT

We present new 3600–2700 cm^{-1} (2.8–3.7 μm) spectra of objects whose extinction is dominated by dust in the diffuse interstellar medium. The observations presented here augment an ongoing study of the organic component of the diffuse interstellar medium. These spectra contain a broad feature centered near 3300 cm^{-1} (3.0 μm) and/or a feature with a more complex profile near 2950 cm^{-1} (3.4 um), the latter of which is attributed to saturated aliphatic hydrocarbons in interstellar grains and is the primary interest of this paper. As in our earlier work, the similarity of the absorption bands near 2950 cm^{-1} (3.4 μm) along different lines of sight and the correlation of these features with interstellar extinction reveal that the carrier of this band lies in the dust in the diffuse interstellar medium (DISM). At least 2.5% of the cosmic carbon in the local interstellar medium and 4% toward the Galactic center is tied up in the carrier of the 2950 cm^{-1} (3.4 μm) band. The spectral structure of the diffuse dust hydrocarbon C—H stretch absorption features is reasonably similar to UV photolyzed laboratory ice residues and is quite similar to the carbonaceous component of the Murchison meteorite. The similarity between the DISM and the meteoritic spectrum suggests that some of the interstellar material originally incorporated into the solar nebula may have survived relatively untouched in primitive solar system bodies. Comparisons of the DISM spectrum to hydrogenated amorphous carbon and quenched carbonaceous composite are also presented. The A_V/τ ratio for the 2950 cm^{-1} (3.4 μm) feature is lower toward the Galactic center than toward sources in the local solar neighborhood ($\sim$150 for the Galactic center sources vs. $\sim$250 for the local ISM sources). A similar trend has been observed previously for silicates in the diffuse medium by Roche & Aitken, suggesting that (1) the silicate and carbonaceous materials in the DISM may be physically correlated and (2) there is either dust compositional variation in the galaxy or galactic variation in the grain population density distribution. We also note a possible absorption feature near 3050 cm^{-1} (3.28 μm), a wavelength position that is characteristic of polycyclic aromatic hydrocarbons (PAHs).

Subject headings: dust, extinction — infrared: ISM: lines and bands

1. INTRODUCTION

Organic materials have previously been detected in the diffuse interstellar medium (DISM) using infrared spectroscopic techniques (cf. Wickramasinghe & Allen 1980; Butchart et al. 1986; Adamson, Whittet, & Duley 1990; Sandford et al. 1991). Organic spectral signatures have also been seen in primitive solar system bodies such as comets, meteorites, and asteroids (cf. Cruikshank & Brown 1987; Tokunaga & Brooke 1990; Cronin & Pizzarello 1990; Brooke, Tokunaga, & Knacke 1991; Mueller et al. 1992). Investigations into the possible connection between the organics in the DISM and primitive solar system bodies are underway (Pendleton 1993, 1994; Pendleton & Cruikshank 1994).

Infrared spectral studies hold the greatest promise for gaining a clear understanding of the chemical identity of organics in the DISM because the fundamental vibrational frequencies of the common chemical bonds between the most cosmically abundant elements occur in the mid-infrared spectral region (5000–400 cm^{-1}; 2–25 μm). Historically, unequivocal identification of the specific molecules responsible for absorption and/or emission features observed in the DISM has met with limited success, in part due to technical constraints on the quality and completeness of astronomical spectra. An additional complication arises from the fact that dust in the interstellar medium undoubtedly contains many different materials having similar chemical function groups. Thus, absorption bands associated with common molecular bonds (e.g., the aliphatic C—H bond) will suffer spectral confusion resulting from band overlap of multiple components.

As a result, it has been possible to "fit" the C—H stretching feature observed toward the Galactic center with a variety of related, but distinctly different, organic materials. These include (1) organic grain mantles consisting of a complex molecular mixture formed by irradiation of ices (cf. Greenberg 1978; d'Hendecourt, Allamandola, & Greenberg 1985; Schutte 1988; Sandford et al. 1991; Khare et al. 1993), (2) hydrogenated amorphous carbons (HACs) having various degrees of hydrogenation (cf. Jones, Duley, & Williams 1987; Borghesi, Bussoletti, & Colangeli 1987), (3) Quenched Carbonaceous composite (QCC), a material produced by quenching the plasma of methane gas (cf. Sakata & Wada 1989), and (4) some less plausible organic materials, such as microorganisms (Hoyle et al. 1982).

An infrared study of the diffuse interstellar medium is underway at NASA's Ames Research Center through a combined effort of infrared observational and laboratory analysis. We have pursued the goal of obtaining high-resolution, high signal-to-noise data through the 3300–2500 cm^{-1} (3.0–4.0 μm)

[1] NASA-Ames Research Center, Mail Stop 245-3, Moffett Field, CA 94035.
[2] NASA-Ames Research Center, Mail Stop 245-6, Moffett Field, CA 94035.
[3] Visiting Astronomer, Infrared Telescope Facility, which is operated by the University of Hawaii under contract with the National Space and Aeronautics Administration.
[4] Department of Astronomy, Ohio State University, 174 West 18th Avenue, Columbus, OH 43210.
[5] Alfred P. Sloan Foundation Research Fellow.

region along different lines of sight that sample dust in the diffuse ISM. Our initial ground-based observational program investigated the detailed nature (peak positions *and* profiles) and the prevalence of the absorption feature near 2950 cm^{-1} (3.4 μm) seen toward the Galactic center and along other lines of sight (Sandford et al. 1991). In Sandford et al. (1991), it was demonstrated that the complex profile of this feature (subfeatures were seen at 2955, 2925, and 2870 cm^{-1}; 3.385, 3.420, and 3.485 μm) can be attributed to the C—H stretching fundamental of $-CH_2-$ and $-CH_3$ groups in aliphatic hydrocarbons that contain other perturbing chemical groups. The feature was detected along various lines of sight not containing dense molecular clouds, and its strength was found to correlate with the amount of interstellar extinction toward these same objects, indicating the carrier resides in the diffuse ISM. It is interesting to note that the C—H stretching feature has now also been detected in a protoplanetary nebula, CRL 618 (Lequeux & Jourdain de Muizon 1990), and in several extragalactic sources, including NGC 1068 (Bridger, Wright, & Geballe 1993) and IRAS 08572 (Wright et al. 1994).

Sandford et al. (1991) reported a relationship of $A_V/\tau = 240 \pm 40$ for the $-CH_2-$ (2925 cm^{-1}) band and $A_V/\tau = 310 \pm 90$ for the $-CH_3$ (2955 cm^{-1}) band, respectively, for their sample of five sources. In this paper we present new observations that increase the number of objects for which the C—H stretching feature has been detected and extended the detection to lower visual extinctions. This allows us to further investigate the A_V/τ relationship for carbonaceous dust in the diffuse ISM.

The high-quality data presented in this paper and in Sandford et al. (1991) also allow us to make more detailed spectral comparisons between dust in the DISM and materials that have been proposed as carriers of the C—H stretching absorption feature. In Sandford et al. (1991) we showed that the profile of the interstellar feature could be well fitted by the spectra of carbonaceous residues produced in laboratory experiments that simulate chemical processing of ices in dense molecular clouds. In this paper we extend such comparisons to include those between the interstellar C—H stretching band and the laboratory spectra of additional photolysis residues, HAC, QCC, E-coli, and an organic extract from the Murchison meteorite. Such comparisons may ultimately help unravel the chemical complexity of the interstellar medium and assist in determining whether any of the organic compounds in primitive solar system bodies originated in the interstellar medium.

Finally, aromatic hydrocarbons are thought to be an important component of the interstellar dust population. Free polycyclic aromatic hydrocarbons (PAHs) are believed to be responsible for the family of interstellar infrared emission features whose strongest bands fall at 3040 cm^{-1} (3.29 μm), 1610 cm^{-1} (6.2 μm), 1300 cm^{-1} (7.7 μm), and 885 cm^{-1} (11.3 μm) (cf. Leger & Puget 1984; Allamandola, Tielens, & Barker 1985, 1989). These small molecules (20–100 C atoms per molecule) are thought to contain $\sim$1% of the carbon in the ISM. Larger molecules and dust grains containing aromatics are not expected to emit the characteristic features of aromatics for energetics reasons (Allamandola et al. 1989), and hence their total abundance is presently not well determined. These materials could potentially be detected in absorption, however. The possibility of detecting absorption in the diffuse medium due to the aromatic C—H stretch near 3040 cm^{-1} (3.29 μm) provides additional incentive for studying the 3300–2500 cm^{-1} region in detail. We will discuss the possible detection of a weak 3040 cm^{-1} (3.29 μm) absorption band in the spectra of Galactic center sources and briefly consider the implications if this detection and identification are correct.

The remainder of the paper is organized as follows. The observation and reduction procedures used to obtain the astronomical data are discussed in § 2, and the resulting data are presented in § 3. The interpretation of the data and comparisons of the interstellar absorption feature with the spectra of various organic materials are presented in § 4. Finally, § 5 contains a summary of our results.

2. OBSERVATIONS AND DATA REDUCTION

All the observations presented here were made at the NASA Infrared Telescope Facility (IRTF) on Mauna Kea using the Cooled Grating Array Spectrometer (CGAS) during 1990 July 25–28. The CGAS employs a linear 32 element InSb detector (Tokunaga, Smith, & Irwin 1987). Output from detectors 1, 2, 13, and 32 was not used as these detectors were not operating reliably during the observation run. We used a 75 line mm^{-1} grating which provided a resolution of 0.018 μm per detector ($\lambda/\Delta\lambda$ = 160–215 over the 3570–2550 cm^{-1} [2.80–3.9 μm] range), and a 300 line mm^{-1} grating which provided a resolution of 0.004 μm per detector ($\lambda/\Delta\lambda$ = 790–880 over the 3020–2700 cm^{-1} [3.31–3.70 μm] range). Wavelength calibration was achieved with an estimated accuracy of about 10% of a resolution element using argon lamp lines. The detector spacing on the CGAS provides one detector per resolution element. The CGAS has a small fixed circular aperture of 2".7 diameter which causes fluctuations in the flux level to occur as a result of seeing or tracking drifts. This can also result in spectral tilts of up to 6%. Our procedure was to obtain spectra with 6–8 detector overlap between grating settings to allow for normalization to compensate for fluctuations in the continuum level between gratings settings. The low-resolution observations required four grating settings to cover the entire 3570–2700 cm^{-1} (2.8–3.7 μm) range. Several observations of each spectral segment were obtained, and the flux level of each one was normalized to the average flux level of that segment. The slope of each observation was forced to match the majority of the observations as well. The four separate spectral segments were then combined into one complete spectrum. The high-resolution observations required two grating settings to cover the 3020–2830 cm^{-1} (3.31–3.53 μm) region. The complete high-resolution spectra were produced in the same manner as the low-resolution spectra. For objects where we had both low- and high-resolution data, the final high-resolution spectrum was tilted to match the slope of the low-resolution spectrum. We estimate the absolute flux levels of our spectra are accurate to within 20%.

Sky subtraction was accomplished by alternately measuring the object and nearby sky by nodding the telescope. Correction for atmospheric absorption and flux calibration was accomplished by comparison with nearby bright stars whose spectra were measured through similar air masses on the same night as the program object (usually within an hour). No further telluric extinction corrections were made to the data since the average air masses of the program objects and their comparison bright stars never differed by more than 0.05 air masses.

A summary of the observational details of the objects and comparison stars discussed here and in Sandford et al. (1991) are summarized in Table 1. Included in the table are the spectral types of the comparison stars. Since *L*-band photometry is not available for most of the comparison stars, the *L* magni-

TABLE 1

SUMMARY OF OBSERVATIONS FROM THIS PAPER AND SANDFORD ET AL. 1991

Object	R.A. (1950)	Decl. (1950)	Comparison Star and Spectral Type[a]	Comparison Star L (mag)	Object Type	Object A_v
GC IRS 7[b]						
Low resolution	$17^h42^m29^s.3$	−28°59′13″.1	BS 6616 (F7II)	2.6	M2I	31
High resolution.....			BS 6616 (F7II)	2.6		
GC IRS 6E						
Low resolution	17 42 28.9	−28 59 04	BS 6616 (F7II	2.6	?[c]	31
High resolution.....			BS 6616 (F7II)	2.6		
GC IRS 3[b].....	17 42 29.1	−28 59 14.9	BS 6616 (F7II)	2.6	MIII	31
HD 229059	20 19 23.0	+37 14 35.0	BS 8028 (A1Vn)	3.86	B1.5Iap	5.3
HD 194279	20 21 33.0	+48 35 48.0	BS 8028 (A1Vn)	3.86	B1.5Iap	3.9
BD +40 4220	20 30 34.8	+41 08 04	BS8028 (A1V)	3.86	O7f	6.2
VI Cygni 12[b]						
Low resolution	20 30 53.4	+41 03 51.6	BS 8028 (A1Vn)	3.86	B5Ia+	10
High resolution.....			BS 8028 (A1Vn)	3.86		
AFGL 2104.....	18 13 37.0	−18 59 49.0	BS 6700 (B9V)	4.9	WC 9	12
AS 320	18 41 34.0	−03 51 04	BS 7236 (B8V)	3.85	WC 9	5.2
AFGL 2179[b]						
Low resolution	18 28 56.8	−10 01 23.3	BS 6812 (B8)	4.07	WC 10	12.8
High resolution.....			BS 7377 (F0IV)	3.65		
Ve 2–45[b]	17 59 00.9	−23 37 35.2	BS 6616 (F7II)	2.6	WC 9	6.5
ST Ceph						
Low resolution	22 28 16	56 44 39	BS 8028 (A1Vn)	3.86	M2	<1
High resolution.....			BS 8494 (F0IV)	3.33		
V 842						
Low resolution	19 11 25	02 23 20	BS 7377 (F0IV)	2.56	M6 + III	<1
High resolution.....			BS 7377 (F0IV)	2.56		

[a] Applies to data taken using the low resolution grating unless otherwise specified.
[b] Object data also discussed in Sandford et al. 1991.
[c] Compact H II region? (see text and Becklin et al. 1978a).

tudes used were determined by ratioing the comparison star data to spectra from BS 8028 (ν Cyg), which was assumed to have an L magnitude of 3.86 (Tokunaga 1986). The derived L magnitudes were then compared to those expected from known V magnitudes and spectral types to ensure the stars being used were spectrally well behaved. Fluxes are based on a 0.0 magnitude flux of 7.3×10^{-11} W m^{-2} μm^{-1} at 3.45 μm (Tokunaga 1986). The resulting calculated fluxes were in reasonable agreement with published photometry for all the objects, where available. Some of the comparison stars used in this work are early-type stars. Their spectra therefore contain hydrogen absorption lines. As a result, these lines appear as "emission" features at 2674 cm^{-1} (Pf γ; 3.740 μm), 3033 cm^{-1} (Pf δ; 3.297 μm), and 3291 cm^{-1} (Pf ϵ; 3.039 μm) in the ratioed spectra. The stellar hydrogen lines are marked on all spectra in which they appear and do not represent spectral features inherent to the lines of sight of interest here.

3. DATA AND RESULTS

3.1. *The Objects and Their Spectra*

We present new observations of Galactic center IRS 6E, VI Cygni 12, and AFGL 2179 at both high spectral resolution ($\lambda/\Delta\lambda$ = 790–880) and low spectral resolution ($\lambda/\Delta\lambda$ = 160–215). We also present new observations of Galactic center IRS 3, HD 229059, HD 194279, BD +40 4220, AFGL 2104, AS 320, and Ve 2-45 at low spectral resolution. For comparison, we also include data from Sandford et al. (1991) for Galactic center IRS 7.

Since we had earlier determined that the photospheric OH lines of M stars can be confused with the C—H stretching band of diffuse ISM dust (Sanford et al. 1991), we also made high-resolution observations of two unobscured M stars. ST Ceph and V842 Aql (Fig. 1), to help us determine the characteristic spectrum of photospheric OH in the C—H stretching region. Comparison of these spectra with the spectra of our other sources allows us to check whether photospheric OH lines are contaminating the diffuse ISM C—H stretch band. It is difficult to assess the absorption contribution of diffuse ISM dust in the C—H stretching region in the spectra of M stars because of their photospheric OH absorption. For this reason, late-type M stars are best avoided as background sources for studies of the diffuse C—H stretching band.

Fluxed spectra of all the objects are presented in Figures 2 and 3. We have also displayed the data in terms of optical depth plots (Figs. 4, 5, and 6) which allows for direct comparisons between the band profiles and strengths of the interstellar, laboratory, and meteoritic spectra. Determining the continuum spectral baseline for conversion of the original fluxed data to optical depth is sometimes ambiguous. In general, for the C—H stretch features, a linear continuum was constructed between the data points near 3100 and 2750 cm^{-1} (3.23 and 3.64 μm), as was done in Sandford et al. (1991). Occasionally other continua were selected. The baselines used to derive the optical depth plots in Figures 4, 5, and 6 are shown as thin solid lines in Figures 2 and 3. For objects in which the C—H feature is superposed on the wing of the broad O—H absorption band centered near 3300 cm^{-1} (GC IRS 3, GC IRS 6E, GC IRS 7, and AFGL 2104), the deduced C—H column densities resulting from such baselines can be underestimated by 20%–50% (see Sandford et al. 1991 for further discussion on baseline choice and its effect on the optical depth spectra). The optical depth spectra contain absorption features that are similar to those identified in Sandford et al. (1991). More detailed descriptions of the objects and their spectra are given in the following sections (§§ 3.2–3.4).

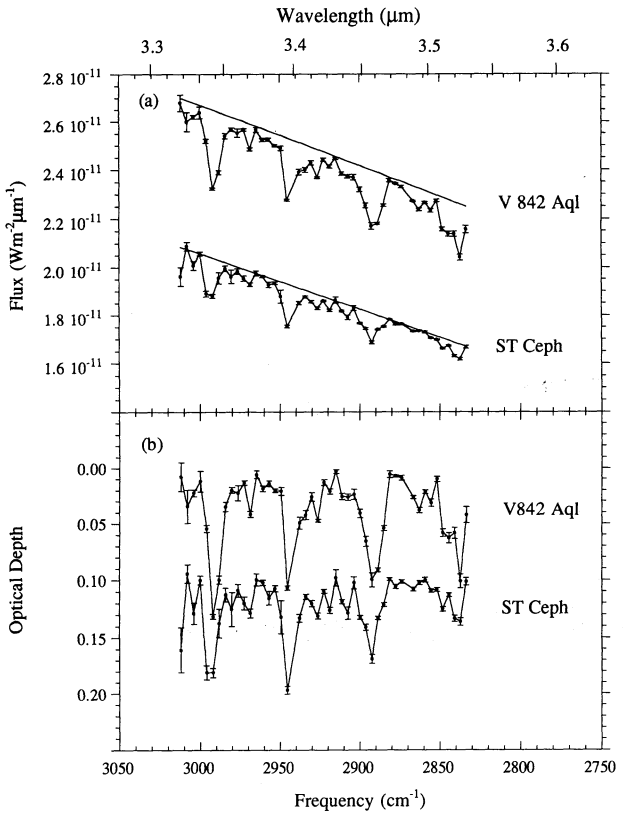

FIG. 1.—The high-resolution (0.004 μm per detector; $\lambda/\Delta\lambda$ = 820–915 over the 3050–2750 cm^{-1} [3.28–3.65 μm] range) spectra of the unobscured M stars ST Ceph and V842 Aql in (*a*) flux, and (*b*) optical depth. The optical depth spectrum was derived using the baselines indicated in (*a*) with solid lines. The sharp absorption lines are due to photospheric OH. In this and all subsequent figures, error bars represent ±1 σ uncertainties. Where error bars are not visible, they are smaller than the points.

3.2. *The Galactic Center (IRS 3, IRS 6E, and IRS 7)*

The new spectra of Galactic center sources GC IRS 3 and GC IRS 6E are shown in Figure 2 (the spectrum of GC IRS 7 is from Sandford et al. 1991). GC IRS 7 is classified as a M2I supergiant (Lebofsky, Rieke, & Tokunaga 1982; Sellgren et al. 1987). The nature of GC IRS 3 is less clear, but it has been suggested that it may be an OH/IR star—an M giant embedded in a circumstellar shell (Becklin et al. 1978a). The classification of GC IRS 6E is also uncertain, as it seems to be part of a more complex source. The overall source GC IRS 6E is known to be extended (Becklin & Neugebauer 1975; Gezari 1992) and high spatial resolution observations at 2.2 μm (DePoy & Sharp 1991), 3.5 μm (Tollestrup, Capps, & Becklin 1989), and 4.8 μm (Gezari 1992) show that GC IRS 6 is a double source at shorter wavelengths. GC IRS 6E is the brighter of the two by about 1.5 mag at *L* and lies 2".9 E and 0".5 S of GC IRS 6W. Becklin et al. (1978a) concluded that GC IRS 6 is most likely a compact H II region whose infrared emission is due to thermal emission by dust heated by an embedded luminosity source.

The interstellar extinction toward the Galactic center is ~31 mag (Becklin et al. 1978b; Henry, DePoy, & Becklin 1984; Sellgren et al. 1987; Wade et al. 1987; Rieke, Rieke, & Paul 1989), although GC IRS 7 shows a total extinction of about 37 mag. The excess extinction toward GC IRS 7 may originate from silicate grains in a circumstellar shell (Rieke et al. 1989). As shown in Figure 2, the strength of the OH feature near 3300 cm^{-1} relative to the C—H feature near 2950 cm^{-1} (3.4 μm) varies among the Galactic center sources IRS 3, 6E, and 7. This confirms the results of an earlier study of the Galactic center by McFadzean et al. (1989), who concluded that the O—H and C—H stretching features in the Galactic center must arise from different carriers. This is also consistent with our conclusions based on previous comparisons between different lines of sight (Sanford et al. 1991). The C—H features in the Galactic center sources IRS 6E and IRS 7 appear quite similar and will be discussed in more detail in §§ 4.2 and 4.3. The optical depth derived from the Galactic center spectra in Figure 2 are shown in Figure 4.

3.3. *Supergiants (HD 229059, HD 194279, BD +40 4220, and VI Cygni 12)*

The HD sources 229059 and 194279 (spectral types B1.5Iap and B1.5Ia, respectively) are located along lines of sight which suffer 5.3 and 3.9 mag of interstellar extinction, respectively (Sneden et al. 1978). BD +40 4220 (also called VI Cygni 3) is an O7f star with A_v = 6.2 mag (Sneden et al. 1978). The hypergiant Cygnus OB 2 no. 12 (VI Cygni 12), classified as B5Ia$^+$ (Humphreys 1978), is a blue hypergiant which is surrounded by a fast (~1400 km s^{-1}), ionized wind ($\Delta M_\odot \approx 4 \times 10^{-5}\ M_\odot$ yr^{-1}; White & Becker 1983). Circumstellar dust that might have formed during a previous evolutionary phase has most likely been swept away by the wind. No evidence for associated infrared emission due to warm dust appears in *IRAS* observations of this object. VI Cygni 12 is located at a distance of only 1.7 kpc, yet has an extinction of A_v = 10 mag. Since the average visual extinction of the diffuse interstellar medium is ~2 mag per kpc, and there are variations of the visual extinc-

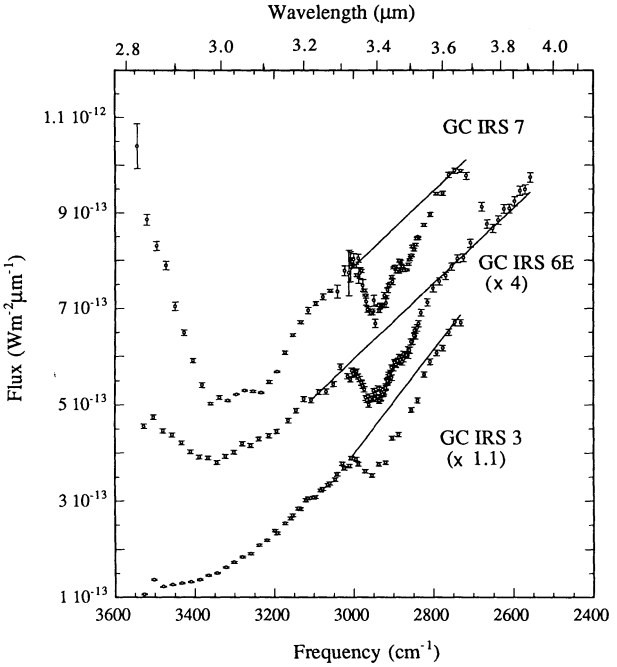

FIG. 2.—The 3600–2400 cm^{-1} (2.78–4.17 μm) fluxed spectra of slight lines toward Galactic center sources IRS 7, IRS 6E, and IRS 3. The low-resolution data have a resolution of 0.018 μm per detector [$\lambda/\Delta\lambda$ = 155–200 over the 3570–2400 cm^{-1} [2.80–4.17 μm] range). High-resolution data points between 3000 and 2820 cm^{-1} (3.33 and 3.55 μm) are superposed for GC IRS 6E and GC IRS 7. The spectra of GC IRS 7 are taken from Sandford et al. (1991).

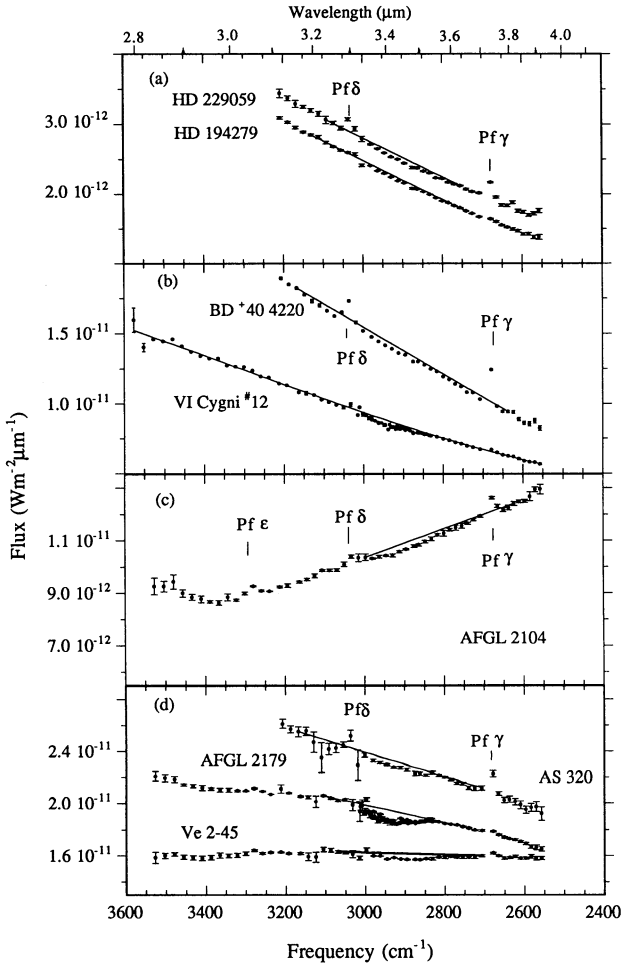

FIG. 3.—The 3600–2400 cm^{-1} (2.78–4.17 μm) low-resolution fluxed spectra of sight lines toward: (*a*) the supergiants HD 229059 and HD 194279, (*b*) the supergiants BD $^{+}$40 4220 and VI Cygni 12, (*c*) the WC star AFGL 2104, and (*d*) the WC stars AS 320, AFGL 2179, and Ve 2-45. High-resolution data points between 3000 and 2820 cm^{-1} (3.33 and 3.55 μm) are superposed for VI Cygni 12 and AFGL 2179. The baselines used to derive optical depth plots are shown as solid lines. Hydrogen Pfund series lines resulting from absorptions in the comparison star spectra are labeled where appropriate.

tion toward other members of the Cyg OB 2 association, some of this extinction is probably associated with local intercluster material. This material may be the remnants of the cloud from which this association formed and which is now being dispersed into the diffuse ISM (Schulte 1958). This is likely to be a general characteristic of all the supergiants, that is, they all may suffer more extinction than expected from the average extinction per kpc in the solar neighborhood. Likewise, because of their short lifetime, they may also still be associated with the remnants of their parental clouds. Fluxed spectra are shown for HD 229059 and HD 194279 in Figure 3*a* and for BD $^{+}$40 4220 and Vi Cygni 12 in Figure 3*b*. We have combined our new low- and high-resolution spectra of VI Cygni 12 with the earlier data from Sandford et al. (1991). Corresponding optical depth plots for all of the fluxed spectra are presented in Figure 5.

As discussed in Sandford et al. (1991), the use of a linear baseline spanning the C—H absorption band region greatly overestimates the strength of C—H feature toward VI Cygni 12 due to the curvature in its fluxed spectrum (Fig. 3*b*). The high- and low-resolution optical depth plots shown for this object in Figure 5*a* were made by assuming a third-order polynomial fit to the continuum rather than a straight line connecting the 3100 and 2750 cm^{-1} points. This method differs slightly from that in Sandford et al. (1991) where an exponential fit was used. The new high-resolution data showed that a polynomial baseline fit the continuum slightly better than did an exponential, but the general shape of the C—H feature remains the same with either choice. The low-resolution C—H feature in the optical depth plot (Fig. 5*a*) closely resembles the C—H feature in the spectra of the Galactic center objects (Fig. 2), as noted in Sandford et al. (1991) for GC IRS 7.

3.4. *WC Stars (AFGL 2104, AS 320, AFGL 2179, and Ve 2-45)*

The objects AFGL 2104, AS 320, AFGL 2179, and Ve 2-45 are Population I, C-rich, Wolf-Rayet stars. They are massive stars ($>20\ M_{\odot}$) which, because of mass loss and mixing, show the products of nucleosynthesis in their photospheres (Abbott & Conti 1987). The spectra of WC stars show evidence for photospheric He, C, and O—approximately in the ratio 10:3:1 by number—but show no evidence for H or N ($<10^{-2}$ and 10^{-3} by number relative to He; Willis 1982; Nugis 1982; Torres 1988). These WC stars produce large infrared emission

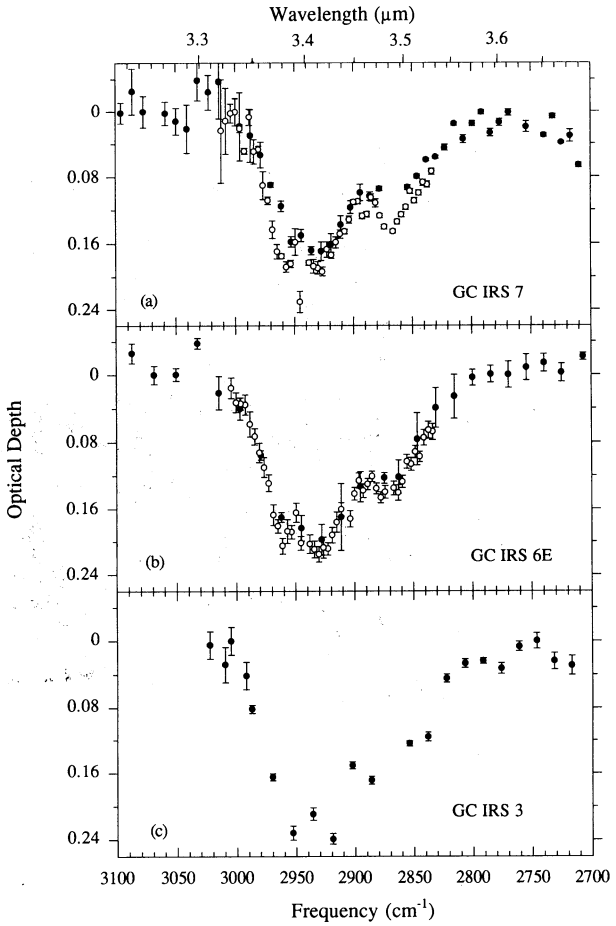

FIG. 4.—Optical depth plots from 3100 to 2700 cm^{-1} (3.2–3.7 μm) for (*a*) GC IRS 7 (taken from Sandford et al. 1991), (*b*) GC IRS 6E, and (*c*) GC IRS 3. High-resolution data are displayed as open points; low-resolution data are displayed as solid points. The baselines used for the derivation of these plots are shown in Fig. 2 as solid lines.

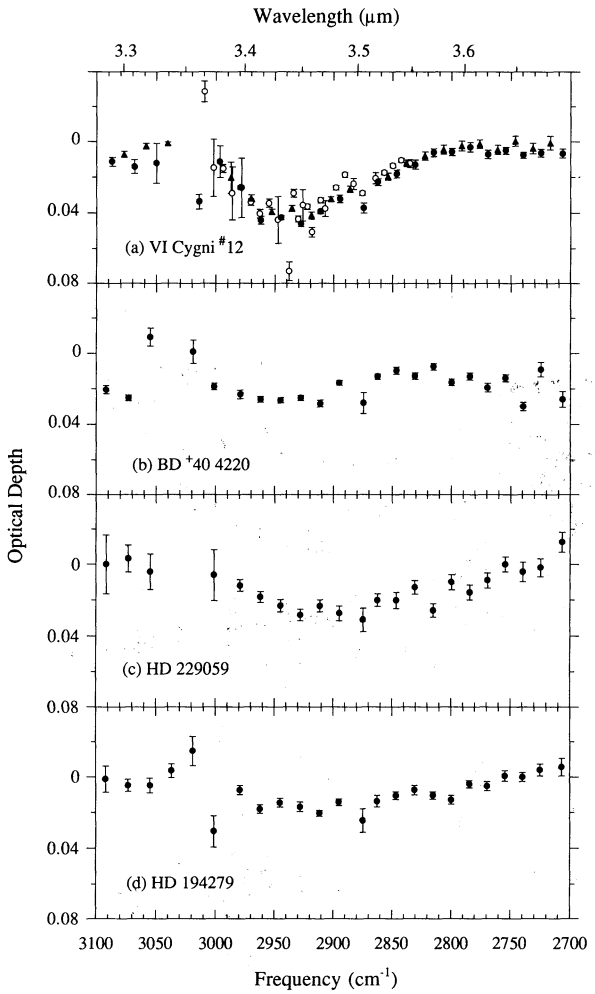

FIG. 5.—Optical depth plots from 3100 to 2700 cm^{-1} (3.2–3.7 μm) for the supergiants (*a*) VI Cygni 12, (*b*) BD +40 4220, (*c*) HD 229059, and (*d*) HD 194279. High-resolution data are displayed as open points; low-resolution data are displayed as solid points. The baselines used for the derivation of these plots are shown in Figs. 3*a* and 3*b* as solid lines. In Fig. 5*a*, the earlier low-resolution VI Cygni 12 data of Sandford et al. (1991) are shown for comparison (*solid triangles*).

excesses thought to be due to carbon grains (Williams, van der Hucht, & Thé 1987), an interpretation supported by the detection of a weak aromatic C—C stretching emission feature near 1300 cm^{-1} (7.7 μm) in the spectrum of Ve 2-45 and AFGL 2104 (Cohen, Tielens, & Bregman 1989).

The total visual extinction toward these objects varies between about 5 and 13 mag, of which the circumstellar shells contribute relatively minor amounts (Cohen & Vogel 1978; Williams et al. 1987). The absence of photospheric H implies that the circumstellar carbon grains associated with these objects cannot produce strong C—H stretching features. Thus, the primary contribution of any C—H absorption in the spectra of these objects probably arises from dust in the intervening diffuse ISM. Our spectra of these WC stars are shown in Figures 3*c* and 3*d*. As with the majority of our objects, a linear baseline across the C—H stretching region was used to produce optical depth profiles for the feature. The baselines used are represented by the solid lines on the fluxed spectra shown in Figures 3*c* and 3*d*, and the resulting absorbance plots can be found in Figure 6.

4. DISCUSSION

4.1. *Absorption Features in the* 3600–2700 cm^{-1} (2.78–3.70 μm) *Region*

A number of molecular vibrations can produce absorption features in the 3600–2700 cm^{-1} (2.78–3.70 μm) region. Considering only the most abundant elements, it is from among the O—H, N—H, and C—H stretching vibrations that we are most likely to find the source(s) contributing to the spectral structure evident in Figures 2–6. A broad ($\Delta\nu \approx 300$ cm^{-1}) feature centered near 3300 cm^{-1} (3.0 μm) generally indicates the presence of O—H stretching in hydrogen-bonding compounds. Bands below 3000 cm^{-1} (longward of 3.3 μm) most likely arise from the C—H stretching vibrations of aliphatic hydrocarbons. The C—H stretch in methane (CH_4) and aromatic hydrocarbons generally fall within 50 cm^{-1} (0.06 μm) of 3050 electrochemical (3.28 μm). It is this mode in telluric atmospheric CH_4 that is responsible for the noise in the spectra near 3000 cm^{-1} (3.3 μm), and which hampers the search for interstellar methane and aromatics near this frequency.

Many of our spectra clearly contain broad absorption features centered near 3300 and/or 2950 cm^{-1} (3.0 and 3.4 μm),

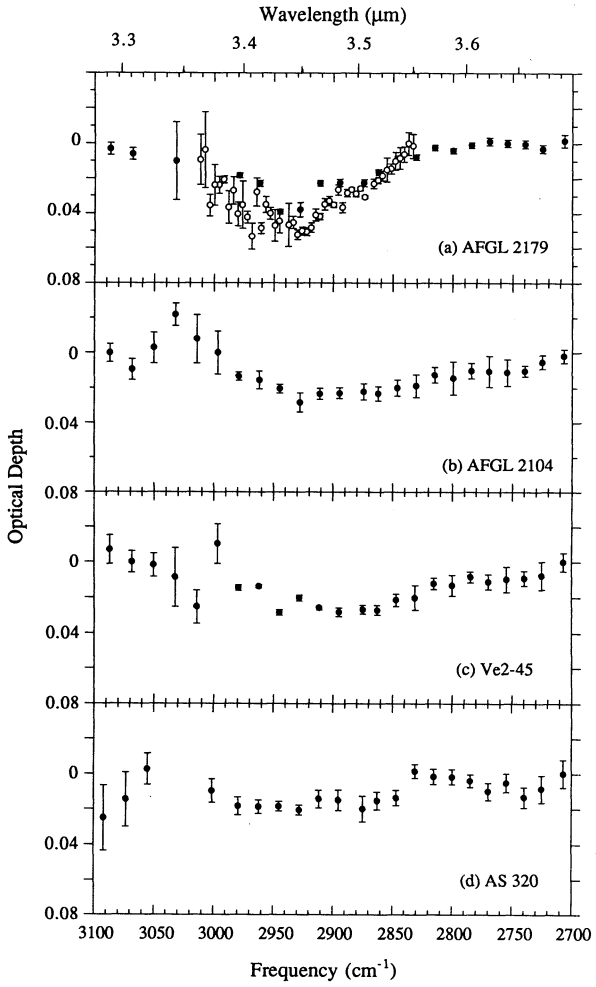

FIG. 6.—Optical depth plots from 3100 to 2700 cm^{-1} (3.2–3.7 μm) for the WC stars (*a*) AFGL 2179, (*b*) AFGL 2104, (*c*) Ve 2-45, and (*d*) AS 320. The baselines used for the derivation of these plots are shown in Figs. 3*c* and 3*d* as solid lines. High-resolution data are displayed as open points; low-resolution data are displayed as solid points.

and, as we discuss later, they may show additional weak features as well. In Sandford et al. (1991), the 3300 cm^{-1} band was attributed to O—H stretching vibrations in nondiffuse ISM materials and the 2950 cm^{-1} band was attributed to the C—H stretching vibrations of aliphatic $-CH_2-$ and $-CH_3$ groups in dust in the diffuse ISM.

The objects in the present paper were chosen to span a wider range of A_v than in Sandford et al. (1991) in order to better test the hypothesis that τ_{CH} and A_v are correlated, especially at lower A_v. Figure 7 shows a plot of the optical depth of the diffuse C—H stretching band (open symbols; as measured by optical depth at 2925 cm^{-1}, 3.42 μm) versus A_v for all our objects. It is apparent that the optical depth of the C—H stretching feature correlates reasonably well with visual extinction toward objects which sample A_v less than 15, supporting the assertion that the organic material is characteristic of the local diffuse ISM, that is, that τ_{CH} arises from dust in the diffuse ISM. The Galactic center sources offer an interesting exception, however. The implications of the difference in the τ_{CH}/A_v relationship toward the Galactic center will be discussed in more detail in a subsequent paper (Sandford, Pendleton, & Allamandola 1994). We note that in the sources that have low values of A_v, the C—H features are so weak that they are not useful for analysis of band positions and profiles. Nonetheless, these sight lines confirm that carbonaceous material is a general characteristic of the diffuse ISM.

4.2. *The Aliphatic Hydrocarbon Component of Dust in the DISM*

The profiles of the C—H stretching features between 3000 and 2800 cm^{-1} (3.33 and 3.57 μm) produced along our various lines of sight are quite similar to those in the spectrum of GC IRS 7. This similarity in profile was previously noted for GC IRS 7 and VI Cygni 12 (Sandford et al. 1991) and provides additional evidence that the C—H absorption in the spectra of these and other objects (Figs. 4, 5, and 6) is due to carbonaceous material in the diffuse ISM. For example, the C—H feature extends from about 3000 to 2800 cm^{-1} in the low-resolution spectra of GC IRS 7 (Sandford et al. 1991; Fig. 4*a*), GC IRS 6E (Fig. 4*b*), and GC IRS 3 (Fig. 4*c*), and the higher resolution spectra of GC IRS 6E and GC IRS 7 both show distinct subfeatures at 2955, 2925, and 2870 cm^{-1} (3.385, 3.420, and 3.485 μm) (Fig. 8).

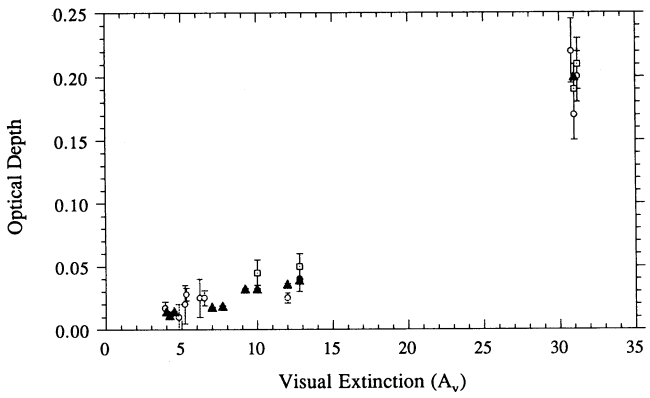

FIG. 7.—Plot of the optical depth of the C—H and Si—O stretching bands due to dust in the diffuse medium vs. optical extinction. The optical depths of the diffuse medium C—H stretching band plotted in the figure were measured at 2925 cm^{-1} (3.42 μm) in the spectra displayed in Figs. 4, 5, and 6 and are shown as open circles (low-resolution data) and open squares high-resolution data). The optical depths of the diffuse medium Si—O stretching silicate band were taken from Roche & Aitken (1984) and are shown as solid triangles. The silicate optical depths have been scaled by a factor of 1/18 to normalize them to the strength of the 2925 cm^{-1} $-CH_2-$ feature at the Galactic center. (The various points associated with the different sources in the Galactic center have been slightly offset from each other in A_v for clarity).

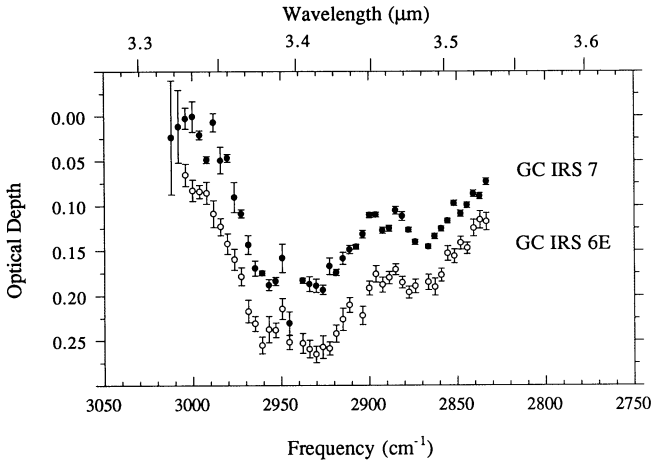

FIG. 8.—A comparison between the high-resolution 3050–2750 cm^{-1} (3.28–3.65 μm) optical depth plots of Galactic center sources IRS 7 and IRS 6E. Note the spectral substructure indicative of $-CH_3$ and $-CH_2-$ groups at 2955 and 2925 cm^{-1}, respectively.

The positions of the 2955 and 2925 cm^{-1} subfeatures are characteristic of the symmetric C—H stretching frequencies of $-CH_3$ (methyl) and $-CH_2-$ (methylene) groups in saturated aliphatic hydrocarbons and the band at 2870 cm^{-1} is characteristic of the asymmetric C—H stretching vibrations of these same functional groups when perturbed by other chemical groups (see Sandford et al. 1991). Given the similarity in profiles of the new high-resolution data shown here and those in Sandford et al. (1991), the new data are consistent with our earlier interpretations. Thus, the carbonaceous material in the diffuse ISM has an average $-CH_2-/-CH_3$ ratio of 2.0–2.5 and likely contains moderate length aliphatic chains, such as $-CH_2-CH_2-CH_3$ and $-CH_2-CH_2-CH_2-CH_3$, associated with electronegative chemical groups, that is, moeities like $-OH$, $-C\equiv N$, and aromatics.

4.3. *Comparison of the Diffuse Medium Dust Spectrum to Spectra of Organic Materials*

Additional understanding of the composition of the carbonaceous carrier in the diffuse ISM can be gained by comparing the interstellar C—H stretching feature with the features produced by other organic materials. Several materials have been suggested as candidate carriers of interstellar carbon. These include hydrogenated amorphous carbon (HAC) (cf. Ogmen & Duley 1988; Adamson et al. 1990), quenched carbonaceous composite (QCC) (cf. Sakata et al. 1987), biological materials (cf. Hoyle et al. 1982), and residues produced by the irradiation of ices (cf. Schutte 1988; Allamandola, Sandford, & Valero 1988; Baratta & Strazzulla 1990; Sandford et al. 1991).

HAC is produced in the laboratory using one of two standard methods: (1) through inefficient hydrocarbon burning in air, and (2) by striking an arc in a controlled Ar atmosphere between two amorphous carbon electrodes (cf. Borghesi et al. 1987; Ogmen & Duley 1988). QCC is synthesized from hydrocarbon (usually methane) plasmas (Sakata & Wada 1989). Figure 9*a* contains a comparison of the spectrum of GC IRS 6E to that of a HAC taken from Borghesi et al. (1987). Figure

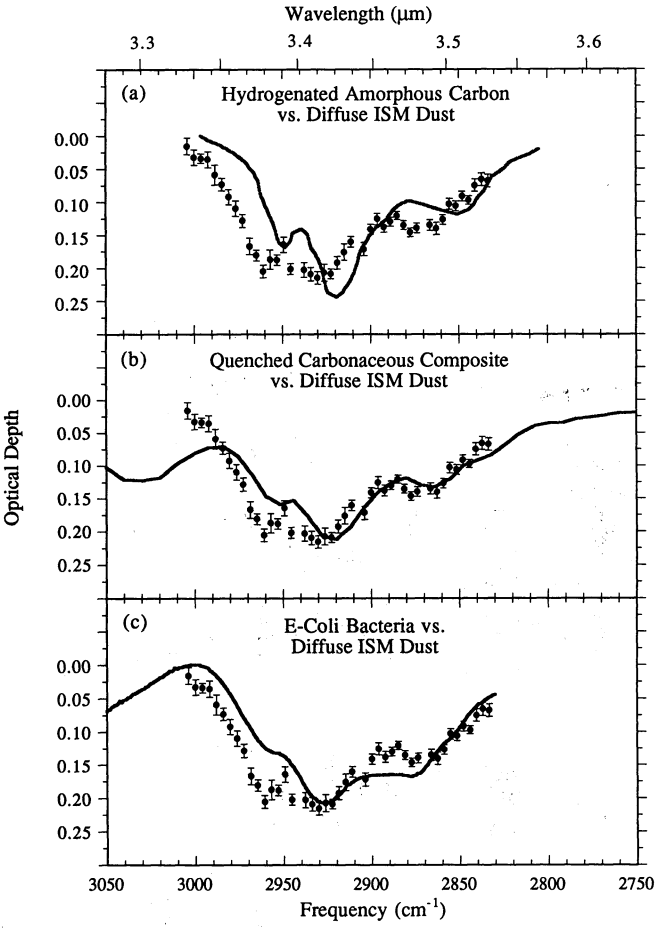

FIG. 9.—A comparison of the optical depth spectrum of Galactic center source IRS 6E (*solid points*) to (*a*) the optical depth spectrum of a room temperature hydrogenated amorphous carbon (HAC) taken from Borghesi et al. (1987; *solid line*), (*b*) the optical depth spectrum of a room temperature filmy quenched carbonaceous composite (QCC) taken from Sakata & Wada (1989; *solid line*), and (*c*) the optical depth spectrum of E-coli suspended in a KBr pellet § 4.3 of this paper; *solid line*).

9*b* contains a similar comparison for QCC which has been heated to 450°C. The QCC spectrum was taken from Sakata & Wada (1989). We compared the GC IRS 6E spectrum to that of QCC at room temperature as well (comparison not shown), but the better match occurred with the heated QCC shown here. Since heating at these temperatures tends to aromaticize the mixture, the better match between the heated QCC and the diffuse ISM is consistent with our conclusion that the diffuse dust contains carbonaceous materials other than aliphatics. It is clear that both HAC and QCC provide a rough match to the interstellar C—H stretching feature, but that both materials produce a feature that differs from the interstellar feature in some details. It is not surprizing that both HAC and QCC fit the interstellar data to first order since both materials contain the $-CH_2-$ and $-CH_3$ functional groups thought to be responsible for the interstellar feature. The detailed differences in the positions and relative strengths of the various subfeatures are largely a reflection of differences in the relative abundances of $-CH_3$, $-CH_2-$, and other chemical groups in the lab materials. For example, the weakness of the subfeature near 2960 cm^{-1} relative to the subfeature near 2925 cm^{-1} in the spectra of HAC and QCC when compared to the same bands in the interstellar feature suggests that the interstellar carrier is richer in $-CH_3$ groups than the particular laboratory HAC and QCC samples shown here. Improved fits could presumably be produced by HACs and QCCs if the relative fractions of their molecular subcomponents were "fine-tuned."

Hoyle et al. (1982) have suggested that the C—H stretching band of diffuse dust may be due to organic materials of biological origin. In particular, they claimed that the spectrum of E-coli provided a good match to the C—H stretching feature in interstellar and cometary spectra. While such an identification seems unlikely (cf. Chyba & Sagan 1987, 1988), we have included a comparison between the spectrum of an E-coli sample and the spectrum of GC IRS 6E for completeness (Fig. 9*c*). Our spectrum of E-coli was taken at a resolution of 1 cm^{-1} using a Nicolet 740 Fourier transform infrared spectrometer. The E-coli sample was prepared using a standard KBr pellet technique (see Sandford 1984 for a description of the sample preparation technique). As with the spectra of HAC and QCC, the spectrum of E-coli is generally similar to the interstellar feature, just as would be expected for *any* material containing abundant aliphatic $-CH_2-$ and $-CH_3$ groups, but differs in detail.

It has previously been shown that the diffuse medium C—H stretching feature is very similar to that produced by residues formed by the UV irradiation and subsequent warming of interstellar ice analogs (Sandford et al. 1991). Infrared spectra of mixed molecular interstellar ice analogs containing H_2O, CH_3OH, CO, and NH_3 reproduce many of the major spectral features attributed to ice in dense clouds (cf. Tielens & Allamandola 1987; Allamandola & Sandford 1988; Allamandola et al. 1988). Ultraviolet photolysis of ices made up of these molecules produces new, more complex compounds. Warming to 150 K leads to the evaporation of the original volatile components of the ices while leaving the more complex C-rich residues behind (see Allamandola et al 1988 and Bernstein et al. 1994a, b for more detailed discussions of the properties of the laboratory photolysis residues produced from CH_3OH-containing ices). Such a process (irradiation followed by warm-up) would be expected to occur to ices in dense molecular clouds that are dispersed into the diffuse ISM by star formation and other dynamic processes.

Figure 10a shows a comparison between the spectrum of GC IRS 6E and that of a residue produced by the UV photolysis and subsequent warm up to 200 K of an $H_2O:CH_3OH:NH_3:CO = 10:5:1:1$ ice. The quality of the fit provided by this laboratory residue is similar to that of the materials discussed earlier, that is, the overall residue feature is similar to the interstellar feature, but differs from it in detail. As with the earlier materials, we note that the lack of a stronger subfeature near 2955 cm^{-1} indicates the abundance of $-CH_3$ groups in the laboratory residue is lower than in the carrier of the interstellar feature. This conclusion is supported by Figure 10*b*, where we show a comparison between the spectra of GC IRS 6E and a laboratory residue produced by the UV photolysis and warm up of an $H_2O:CH_3OH:NH_3:CO:C_3H_8 = 10:5:1:1:1$ ice, that is, an ice enriched in $-CH_3$ groups relative to the one shown in Figure 10*a*. The resulting laboratory spectrum provides an improved fit to the diffuse medium C—H stretching feature.

We note that such fits are not restricted to ices irradiated by UV photons. Similar spectral fits can be obtained when the irradiation of the ice is provided by ionizing particles. Figure 10*c* shows an example of the fit provided by an organic residue

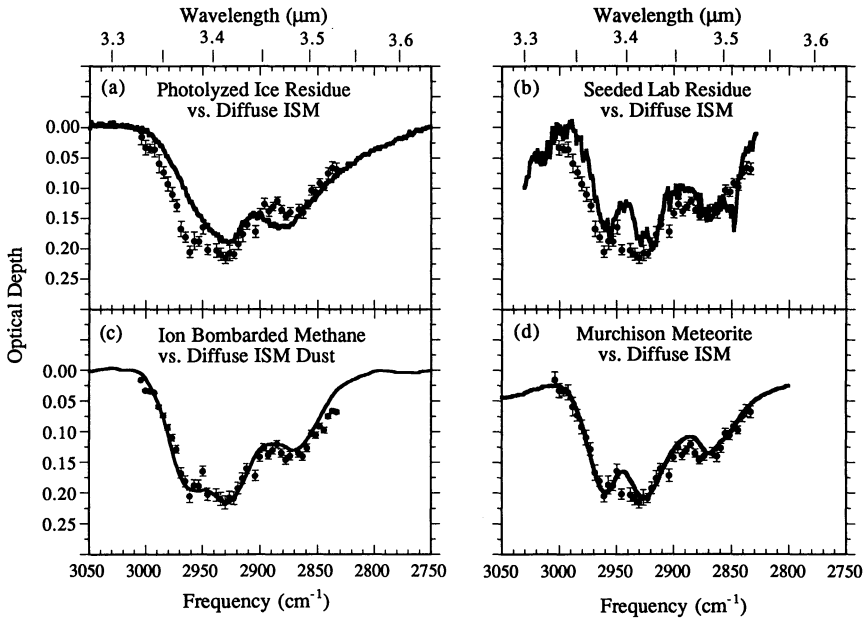

FIG. 10.—A comparison of the optical depth spectrum of Galactic center source IRS 6E (*solid points*) to (*a*) the spectrum of a laboratory residue produced by the UV irradiation of a 10 K H_2:CH_3OH:NH_3:CO = 10:5:1:1 interstellar ice analog followed by warm-up at 200 K (*solid line*), (*b*) the spectrum of a laboratory residue produced by the UV irradiation of a 10 K H_2O:CH_3OH:NH_3:CO:C_3H_8 = 10:5:1:1:1 interstellar ice analog followed by warm-up to 200 K (*solid line*), (*c*) the spectrum of a laboratory residue produced by irradiating frozen (10 K) methane ice with a 180 eV/C-atom dose of 75 keV protons (*solid line*), and (*d*) the spectrum of an organic Murchison acid residue (*solid line*). The photolysis residue spectra in (*a*) and (*b*) were taken from Allamandola et al. (1988), the spectrum of irradiated methane was kindly provided by G. Strazzulla, and the meteoritic spectrum was taken from De Vries et al. (1993) and was kindly provided by W. Golden.

produced by irradiating a 10 K methane ice with 75 keV protons to a total dose of 180 eV/C-atom (spectrum kindly provided by G. Strazzulla).

Some of the hydrocarbon components in primitive meteorites show strong deuterium enrichments and other isotopic anomalies that indicated a connection of interstellar grains and molecules (Kerridge 1987; Kerridge, Chang, & Shipp 1987; Ming & Anders 1988; De Vries et al. 1993; Amari, Lewis, & Anders 1994; Lewis, Amari, & Anders 1994). The presence of isotropically anomalous diamonds, SiC, TiC, and graphite in meteorites confirms that some interstellar materials were incorporated into meteorites and survived subsequent processing on the meteorite parent bodies (cf. Anders & Zinner 1993). If the same were true for the organic component of interstellar dust, then the carbonaceous materials observed in the diffuse ISM may be one of the "parent" components from which the carbonaceous material in meteorites was derived.

Earlier comparisons of the spectra of the organic residue found in solvent soluble, acid insoluble extracts of the primitive CM meteorite Murchison with the interstellar C—H stretching feature showed a strong similarity (Ehrenfreund et al. 1991). This comparison was made prior to the availability of the high-resolution, high signal-to-noise spectra of the diffuse ISM, and the recent high-quality meteoritic spectra of De Vries et al. (1993). Figure 10*d* shows a comparison between our spectrum of GC IRS 6E and the spectrum of an organic component of the Murchison chondrite taken by De Vries et al. The two spectra in Figure 10*d* are remarkably similar to peak positions, widths, and profiles. Since the organic material in primitive meteorites is dominated by a macromolecular "kerogen" which consists largely of abundant aromatic moeities interlinked by short aliphatic bridges (Hayatsu & Anders 1981; Mullie & Reisse 1987), this match is entirely consistent with the suggestion of Sandford et al. (1991) that the diffuse ISM material consists of the short aliphatic chains attached to electronegative or other perturbing groups. The match presented in Figure 10*d* suggests that aromatic materials may be the dominant form of perturbing group present.

Another interesting comparison to the carbonaceous component of the Murchison meteorite has recently been made by Lee & Wdowiak (1993), who obtained the spectrum of a residue produced by passing a discharge through a gaseous mixture of hydrogen and the polycyclic aromatic hydrocarbon naphthalene ($C_{10}H_8$). The spectrum of their residue provides a good overall match to the meteoritic data throughout the mid-infrared region but, like all the other laboratory materials discussed above, their residue appears to have a higher ratio of $-CH_2-$ to $-CH_3$ groups than the carrier of the interstellar feature. Therefore, while the spectral fit of their residue to the meteoritic data is quite impressive and provides additional support for the idea that the interstellar carrier contains aromatic materials, it does not provide as compelling a match to the interstellar C—H stretching feature as does the meteoritic material itself.

Several points can be made from the comparisons shown in Figures 9 and 10. First, as has long been known, *any* material that contains substantial amounts of aliphatic $-CH_2-$ and $-CH_3$ groups will produce a feature whose overall position and profile is similar to that of the diffuse interstellar C—H stretching feature. Thus, the general fits provided by all the spectra in Figures 9 and 10 support the idea that dust in the diffuse medium contains abundant aliphatic $-CH_2-$ and $-CH_3$ groups. In this regard, however, it is unlikely that comparisons between astronomical and laboratory data in this spectral region will ever yield a "unique" identification of the interstellar carrier. It is also clear that many of the analog materials proposed as the carriers of the interstellar feature on the basis of their fits to older, low-resolution astronomical data

do not fit the details of the actual profile of the interstellar feature as determined by the high-resolution data given here and in Sandford et al. (1991). High signal-to-noise, high-resolution ($\Delta\lambda/\lambda \geq 750$) astronomical data therefore represent a means by which the spectral properties of various laboratory materials can be used to further constrain the chemical composition of the carrier of the diffuse C—H stretching feature. This illustrates the need for both additional high-resolution, full spectral coverage, high-quality data like that of GC IRS 6E presented here and corresponding spectroscopic laboratory data from additional, relevant, well-characterized materials have a range of appropriate compositions.

In summary, the best match to the overall interstellar C—H stretching feature is provided by the carbonaceous fraction of the Murchison meteorite (Fig. 10*d*) and, to a somewhat lesser extent, the residues produced by the UV photolysis of some ice mixtures (Fig. 10*b*). While this does not prove that these specific materials are responsible for the diffuse medium C—H absorption band, it does imply that they contain relative abundances of $-CH_3$, $-CH_2-$, and perturbing chemical groups that are similar to those in the carbonaceous dust population in the diffuse ISM. Thus, even if they are not identical to the carrier of the interstellar feature, they may be good potential analogs for the composition of the diffuse dust.

4.4. *Relationships to Visual Extinction, Column Densities, and Abundances*

As discussed in § 4.1, the τ_{CH} vs. A_v plot shown in Figure 7 demonstrates that the optical depth of the C—H stretching feature at 2925 cm^{-1} correlates reasonably well with visual extinction along lines of sight that sample the local interstellar neighborhood ($A_v < 15$). This supports the assertion that the material responsible for the C—H stretching band resides in the diffuse ISM. In view of the good peak position and profile match of the interstellar 2955 and 2925 cm^{-1} subfeatures to those produced by saturated aliphatic hydrocarbons, the known spectroscopic properties of these compounds can be used to quantitatively analyze the interstellar features. The column density, N (molecules cm^{-2}), of material producing an infrared absorption feature can be determined from

$$N = \frac{\int \tau(\nu) d\nu}{A} \approx \frac{(\tau_{max} \Delta\nu_{1/2})}{A}, \quad (1)$$

where $\tau(\nu)$ is the frequency-dependent optical depth, τ_{max} is the maximum optical depth of the feature of interest, $\Delta\nu_{1/2}$ is the full width at half maximum (in cm^{-1}) of the band from absorbance spectra, and A is the integrated absorbance in cm molecule^{-1} (see d'Hendecourt & Allamandola 1986 and Hudgins et al. 1993 for A values relevant to many interstellar materials). We have used equation (1) to calculate column densities of $-CH_2-$ and $-CH_3$ associated with the τ_{max} values for the 2955 and 2925 cm^{-1} asymmetric C—H stretching bands in the spectra shown in Figures 4, 5, and 6. See Sandford et al. (1991) for additional details on this procedure.

The column densities of $-CH_2-$ and $-CH_3$ groups are summarized in Table 2 and were derived using the A and $\Delta\nu_{1/2}$ values from Table 4 in Sandford et al. (1991) and the τ_{CH} values given here in Table 2. Table 3 provides a summary of the column densities compared to A_v, the optical depth of the silicate feature near 10 μm, and the column densities of H and C along the same lines of sight. The H and C column densities were calculated assuming $N(H) = 1.9 \times 10^{21} A_v$ (Bohlin, Savage, & Drake 1978) and $N(C)/N(H) = 3.7 \times 10^{-4}$ (Allen 1973). Sandford et al. (1991) reported A_v/τ values of $A_v/\tau_{(2925\ cm^{-1})} = 240 \pm 40$ and $A_v/\tau_{(2955\ cm^{-1})} = 310 \pm 90$. Our larger data set, which extends to lower A_v and provides reduced uncertainties, is in good agreement with these values. We find average values for the local diffuse ISM to be $A_v\tau_{(2925\ cm^{-1})} = 250 \pm 40$ and $A_v/\tau_{(2955\ cm^{-1})} = 270 \pm 40$ (Table 2).

It is apparent from both Figure 7 and Table 2 that the A_v/τ_{CH} ratios are significantly lower for sources in the Galactic center than for closer sources. This point was noted briefly by Sandford et al. (1991) but not pursued. Our larger data set confirms this difference. Further, we note that the difference between the local diffuse ISM and the Galactic center A_v/τ_{CH} ratio seems to be a factor of about 2, the same factor observed for silicates in the diffuse ISM by Roche & Aitken (1984). Indeed, in Figure 7 we have plotted the optical depths of the Si—O stretching band near 1030 cm^{-1} (9.7 μm) of diffuse medium silicates (filled triangles; from Aitken & Roche 1984; scaled downward by a factor of 18) on top of our combined $\tau_{(2925\ cm^{-1})}$ data (open symbols), and the similarities in their A_v/τ relations are striking. This implies that the grains responsible for the diffuse medium aliphatics C—H and silicate Si—O stretching bands are different from those responsible for the observed visual extinction (or at least they are not solely responsible for the visual extinction). It also suggests that the distribution of this C—H carrier is not uniform throughout the Galaxy, but may instead increase in density toward the center of the Galaxy. The matching behavior of the C—H and Si—O stretching bands suggests that these two components may be coupled, perhaps in the form of silicate core, organic mantle grains. The implications of this match are too extensive to be addressed in any detail here, and the interested reader is referred to Sandford, Pendleton, & Allamandola (1994), where different model distributions of these materials are used to quantitatively explore the possible meanings of the A_v/τ relationship.

Table 3 shows that the lower limit to the fractional abundance of C in the combined aliphatic $-CH_2-$ and $-CH_3$ components of the diffuse dust is about 2.5% in the solar neighborhood and about 4% toward the Galactic center. In the case of the Galactic center, this may only be a rough value for the fraction of cosmic carbon tied up in $-CH_2-$ and $-CH_3$ groups. The strengths of the C—H stretching bands toward the Galactic center are probably underestimated because our choice of baselines almost certainly overestimates the contribution due to the O—H component in this wavelength region, so more aliphatic groups may actually be present (see Sandford et al. 1991 for further discussion of this point. On the other hand, the percentage of C calculated for the Galactic center assumes that standard $A_v/N(H)$ and $N(H)/N(C)$ relations apply along the entire line of sight. Since the standard $A_v/N(H)$ relationship may not hold for the Galactic center (see above and Sandford et al. 1994), and since the Galactic center probably has a higher metallicity, that is, a lower $N(H)/N(C)$ ratio, the total C column density along this line of sight may actually be larger than that used here. These two uncertainties (baseline and metallicity) operate in opposite directions and result in a correspondingly cruder estimate of the fraction of C tied up in the aliphatic component of the dust toward the Galactic center.

4.5. *Are Aromatic Hydrocarbons Present?*

Polycyclic aromatic hydrocarbons (PACs) are thought to be ubiquitous in space and are likely to be responsible for the infrared emission features seen in the spectra of many Galactic

TABLE 2

OPTICAL DEPTH AND COLUMN DENSITIES ASSOCIATED WITH METHYL ($-CH_3$) AND METHYLENE ($-CH_2-$) DIFFUSE INTERSTELLAR MEDIUM DUST COMPONENTS AND RELATION TO A_v[a]

Object[b]	Parameters	$-CH_3$ (2955 cm^{-1})	$-CH_2-$ (2925 cm^{-1})
GC IRS 7 ($A_v = 31$)	υ	2953	2973
(low resolution)	τ	0.16	0.17
	N	2.4×10^{17}	5.0×10^{17}
	A_v/τ	195	180
GC IRS 7 ($A_v = 31$)	υ	2957	2926
(high resolution)	τ	0.19	0.19
	N	2.8×10^{17}	5.7×10^{17}
	A_v/τ	165	165
GC IRS 6E ($A_v = 31$).....	υ	2961	2928
(low resolution)	τ	0.17	0.20
	N	2.6×10^{17}	6.0×10^{17}
	A_v/τ	180	155
GC IRS 6E ($A_v = 31$).....	υ	2961	2926
(high resolution)	τ	0.205	0.21
	N	3.1×10^{17}	6.2×10^{17}
	A_v/τ	150	150
GC IRS 3 ($A_v = 31$)	υ	2953	2919
(low resolution)	τ	0.23	0.24
	N	3.5×10^{17}	7.1×10^{17}
	A_v/τ	135	130
HD 229059 ($A_v = 5.3$)	υ	2945	2928
(low resolution)	τ	0.023	0.028
	N	3.5×10^{16}	8.4×10^{16}
	A_v/τ	230	190
HD 194279 ($A_v = 3.9$)	υ	2945	2928
(low resolution)	τ	0.015	0.017
	N	2.0×10^{17}	5.0×10^{17}
	A_v/τ	260	230
BD $+40$ 4220 ($A_v = 6.2$)	υ	2945	2928
(low resolution)	τ	0.027	0.025
	N	4.0×10^{16}	7.5×10^{17}
	A_v/τ	230	245
VI Cygni 12 ($A_v = 10$)	υ	2945	2928
(low resolution)	τ	0.043	0.046
	N	6.4×10^{16}	1.36×10^{17}
	A_v/τ	230	220
VI Cygni 12 ($A_v = 10$)	υ	2963	2930
(high resolution)	τ	0.04	0.043
	N	6.0×10^{16}	1.3×10^{17}
	A_v/τ	250	230
AFGL 2104 ($A_v = 12$)	υ	2945	2928
(low resolution)	τ	0.037	0.044
	N	5.6×10^{16}	1.3×10^{17}
	A_v/τ	325	275
AFGL 2179 ($A_v = 12.8$)	υ	2945	2930
(low resolution)	τ	0.04	0.038
	N	6×10^{16}	1.13×10^{17}
	A_v/τ	320	335
AFGL 2179.....	υ	2950	2930
(high resolution)	τ	0.05	0.052
	N	7.5×10^{16}	1.5×10^{17}
	A_v/τ	255	245
AS 320 ($A_v = 5.2$)	υ	2944	2928
(low resolution)	τ	0.018	0.02
	N	2.7×10^{16}	5.9×10^{16}
	A_v/τ	290	260
Ve 2-45 ($A_v = 6.5$).....	υ	2945	2928
(low resolution)	τ	0.02	0.02
	N	4.2×10^{16}	6.0×10^{16}
	A_v/τ	325	325
Average values for local ($A_v < 15$) DISM[c]	A_v/τ	270 ± 40	250 ± 40
Average DISM values toward Galactic center[c].....	A_v/τ	150 ± 15	150 ± 20

[a] Units are: υ (cm^{-1}); N (groups/cm^2); band positions accurate to 5 cm^{-1}; uncertainty in τ is dominated by uncertainties in the baselines underlying the features (see text) and is ~20%–30%. N was derived from $A_{CH2} = 7.4 \times 10^{18}$ cm/CH_2 group, $\Delta\nu_{CH2} = 22$ cm^{-1}, $A_{CH3} = 1.2 \times 10^{-17}$ cm/CH_3 group, and $\Delta\nu_{CH3} = 18$ cm^{-1} (d'Hendecourt & Allamandola 1986; Sandford et al. 1991).

[b] Listed A_v values represent best estimates of the extinction due only to the diffuse interstellar material. All extinctions are in units of magnitudes.

[c] Where high-resolution data were available, average values of A_v/τ were calculated neglecting low-resolution data.

TABLE 3

HYDROGEN, CARBON, $-CH_3$, AND $-CH_2-$ COLUMN DENSITIES, AND THE PERCENT OF COSMIC CARBON IN THE ALIPHATIC HYDROCARBON COMPONENT OF DIFFUSE MEDIUM DUST

Object	A_v	τ(sil)[a]	N(H)[b]	N(C)[b]	$N(CH_3)$	$N(CH_2)$	Percentage C[c]
GC IRS 7 (high resolution)	31	3.6 ± 0.4	5.9×10^{22}	2.2×10^{19}	2.9×10^{17}	5.7×10^{17}	3.9%
GC IRS 6E (high resolution)	31	3.6 ± 0.4	5.9×10^{22}	2.2×10^{19}	3.1×10^{17}	6.2×10^{17}	4.2
GC IRS 3	31	3.6 ± 0.4	5.9×10^{22}	2.2×10^{19}	3.5×10^{17}	7.1×10^{17}	4.9
HD 229059	5.3	...	1.0×10^{22}	3.7×10^{18}	3.5×10^{16}	8.5×10^{16}	3.2
HD 194279	3.9	...	7.4×10^{21}	2.7×10^{18}	2.0×10^{16}	5.0×10^{16}	2.6
BD +40 4220	6.2	...	1.2×10^{22}	4.4×10^{18}	4.0×10^{16}	7.5×10^{16}	2.6
VI Cygni 12 (high resolution)	10	0.58 ± 0.1	1.9×10^{22}	7.0×10^{18}	6.0×10^{16}	1.3×10^{17}	2.7
AFGL 2104	12.0	...	2.3×10^{22}	8.4×10^{18}	5.6×10^{16}	1.3×10^{17}	2.2
AS 320	5.2	0.26	9.9×10^{21}	3.7×10^{18}	2.7×10^{16}	6×10^{16}	2.4
AFGL 2179 (high resolution)	12.8	...	2.4×10^{22}	9.0×10^{18}	7.0×10^{16}	1.6×10^{17}	2.6
Ve 2-45	6.5	...	1.2×10^{22}	4.6×10^{18}	4.6×10^{16}	6.0×10^{16}	2.2

[a] Silicate optical depths were taken from Roche & Aitken 1984.

[b] N(H) and N(C) were calculated assuming $N(H) = 1.9 \times 10^{21} A_v$ (Bohlin et al. 1978) and $N(C)/N(H) = 3.7 \times 10^{-4}$ (Allen 1973).

[c] This is a lower limit for the percent of cosmic carbon which is tied up in the $-CH_3$ and $-CH_2-$ groups combined ($[N(CH_3) + N(CH_2)]/N(C)$).

and extragalactic objects (cf. Leger & Puget 1984; Allamandola et al. 1985, 1989; and references therein). Broader emission bumps underlying these narrower emission features are generally interpreted as being due to clusters of PAHs or amorphous carbon particles rich in aromatics (see Witteborn et al. 1989; Allamandola 1991; and references therein). There is also tentative evidence for an absorption feature near 3080 cm^{-1} (3.25 μm) in the spectra of dense molecular clouds, which, if confirmed, may be due to PAHs (Sellgren, Smith, & Brooke 1994). In addition, a significant fraction of the carbon in meteorites is also in the form of aromatics (cf. Hayatsu & Anders 1981; Basile, Middleditch, & Oro 1984; Mullie & Reisse 1987). The aromatics in meteorites are often enriched in deuterium (Krishnamurthy et al. 1992; Cronin & Chang 1994), indicating a possible interstellar connection. Given the ubiquity of aromatics suggested by the various astronomical data and the good spectral match to the aliphatic C—H stretching feature of dust in the diffuse ISM provided by the aromatic-rich carbonaceous component of primitive meteorites (§ 4.3; Fig. 10*d*), a search for aromatic spectral signatures in absorption in diffuse medium dust is clearly in order.

The C—H stretching absorption feature of aromatic hydrocarbons falls near 3050 cm^{-1} (3.28 μm), the exact position depending on the molecule in question. A mixture of aromatics would then be expected to produce a band centered near 3050 cm^{-1} (3.28 μm). Examination of Figure 2 shows that there may be some weak absorption present near 3050 cm^{-1} in the fluxed spectra of GC IRS 7, GC IRS 6E, and GC IRS 3. The potential presence of a weak hydrogen Pfδ line at 3040 cm^{-1} (3.29 μm) in the comparison star spectra used and strong telluric methane lines in this same region make a definitive detection of the 3050 cm^{-1} band difficult.

If this feature is real in the Galactic center spectra, its optical depth as a *discrete* feature is less than 0.02 (we remind the reader that, just as is the case with the aliphatic C—H stretching band, some of the absorption in the overlying low-frequency "wing" of the O—H stretching feature in these spectra may actually be associated with carbonaceous materials). Compared to the aliphatic bands, only a weak aromatic feature is expected since aromatics contain fewer H atoms per C atom (H/C < 1) than do aliphatics (H/C > 2) and because the intrinsic strength of the aromatic C—H stretching band is 2–3 times lower than its aliphatic counterpart. The integrated strength of the potential *discrete* 3050 cm^{-1} aromatic feature in the Galactic center spectra is $\int \tau\, dv \approx 1$ cm^{-1}. With an intrinsic integrated strength of $A_{CH} = 8 \times 10^{-19}$ cm per aromatic C—H group, this translates into a column density of $\sim 1 \times 10^{18}$ H atoms per cm^2 attached to aromatic structures toward the Galactic center, that is, to an aromatic C column density of 1×10^{18} cm^{-2}. Adopting standard dust-to-gas ratios ($N_H/A_v = 2 \times 10^{21}$ cm^{-2}/mag), the total H column density toward the Galactic center is about 6×10^{22} cm^{-2}, implying a total C column density of 2×10^{19} cm^{-2}. Hence, if the 3050 cm^{-1} feature is real, $\sim 5\%$ of all the carbon along the line of sight is tied up in the aromatic carbons attached to hydrogen atoms.

Given that aromatic molecules contain carbon atoms not bonded to hydrogen and that any aromatic moieties bound in carbon grains will have lost some of their peripheral hydrogen to bonding with interlinking aliphatics, this fraction (5%) would represent a lower limit to the aromatic carbon present. If the interstellar material is similar to meteoritic kerogen, we estimate that the aromatic abundance fraction could well be $\sim 10\%$ of the C along the line of sight to the Galactic center. This is much larger than estimated from objects that show the IR emission features (C about 1%; Leger & Puget 1984; Allamandola et al. 1985, 1989), suggesting that more aromatic carbon exists in large PAHs, PAH clusters, and aromatic grains than in the form of gas phase molecules. Given that approximately 2.5% of the carbon in the diffuse medium is in the form of aliphatics (Sandford et al. 1991; Table 3 of this paper), these numbers indicate that these materials could have aromatic to aliphatic C abundance ratios greater than five. Such a ratio is entirely consistent with that observed in meteoritic kerogens.

Given the large potential abundance of aromatics implied, it is clearly important to resolve the issue of the presence of the 3050 cm^{-1} absorption feature in diffuse medium dust. In this

regard, we note two possible approaches that may be worth pursuing. First, it may be possible to detect absorption bands in the 900–700 cm^{-1} (11–14 μm) region due to the out-of-plane C—H bending mode vibrations of aromatics in diffuse dust. These modes are generally stronger than the C—H stretching modes in the spectra of neutral PAHs and so may be easier to detectable. The detection of the aliphatic C—H stretching feature in the galaxy IRAS 08572 (Wright et al. 1994) opens up a second possibility. This galaxy is far enough away that its cosmological redshift ($\sim$150 cm^{-1}; 0.2 μm) is large enough that the aromatic absorption feature would fall in the vicinity of 2900 cm^{-1} (3.45 μm), a spectral position not complicated by atmospheric methane absorptions and hydrogen Pfδ lines of comparison stars that make the search in Galactic sources so difficult. Thus, detection of an absorption band due to aromatic C—H stretching vibrations may be more easily done using observations of external galaxies.

5. CONCLUSIONS

Interstellar spectra in the 3600–2700 cm^{-1} (2.8–3.7 μm) region generally contain either a broad absorption feature near 3300 cm^{-1} (3.0 μm), a broad complex absorption feature centered near 2950 cm^{-1} (3.4 μm), or both. The feature near 2950 cm^{-1} is attributed to C—H stretching vibrations in aliphatic materials. We have presented observations of a variety of lines of sight within our Galaxy that show evidence that the absorption feature near 2950 cm^{-1} (3.4 μm) arises from material in the diffuse ISM. This result is in agreement with the earlier conclusions of Sandford et al. (1991), but is based on the observations of a larger number of sight lines that extend the range to lower extinctions.

A new high resolution spectrum of the interstellar C—H stretching feature toward Galactic center source IRS 6E contains subpeaks near 2955, 2925, and 2870 cm^{-1} (3.385, 3.420, and 3.485 μm), positions characteristic of C—H stretching vibrations in the $-CH_3$ and $-CH_2-$ groups of saturated aliphatic hydrocarbons associated with perturbing chemical groups. The overall profile of this band is in good agreement with that obtained from Galactic center source IRS 7 by Sandford et al. (1991). Thus, we confirm their conclusions that the diffuse ISM carrier of this feature has an average $-CH_2-/-CH_3$ ratio of 2.0–2.5, implying that it must contain relatively complex organic materials containing short aliphatic chains. At least 2.5% of the cosmic C in the local ISM is tied up in solid aliphatic materials.

The abundance of the material is correlated with visual extinction. We find that the local diffuse ISM can be well described by the relationships $A_v/\tau_{(2925\ cm^{-1})} = 250 \pm 40$ and $A_v/\tau_{(2955\ cm^{-1})} = 270 \pm 40$. These relationships are consistent with those reported by Sandford et al. (1991), but we show that they extend to lower values of extinction. In contrast, we find that the A_v/τ_{CH} ratio is smaller toward the Galactic center ($A_v/\tau_{(2925\ cm^{-1})}$ and $A_v/\tau_{(2955\ cm^{-1})} \approx 150$). The implications of this difference are discussed elsewhere (Sandford et al. 1994).

Comparison of the diffuse interstellar C—H band profiles with the spectra of laboratory samples of candidate analog materials, including hydrogenated amorphous carbon (HAC), quenched carbonaceous composite (QCC), E-coli, the organic residue produced by the UV photolysis of interstellar ice analogs, and a carbonaceous fraction of the primitive CM meteorite Murchison, all show general similarities to the interstellar C—H stretching feature. This is undoubtedly because all of these materials contain significant aliphatic $-CH_2-$ and $-CH_3$ fractions. Comparisons with our best astronomical data show that the available spectra of many of these materials fail to fit the interstellar feature in all details, suggesting that they do not yet contain the exact mixture of molecular components present in the carbonaceous fraction of the dust in the diffuse ISM. This stresses the need for both additional high-resolution, high signal-to-noise astronomical data and additional laboratory data from a variety of materials spanning a greater composition range. The best fit to the interstellar C—H stretching feature were provided by the spectrum of a carbonaceous fraction of the primitive carbonaceous chondrite Murchison. Although it does not prove it, this suggests that the carbonaceous component of dust in the diffuse ISM and the meteoritic material may be closely related and that the carbonaceous fraction of primitive meteorites may represent the best analog material presently available for the organic fraction of the dust in the diffuse ISM.

We have also reported the tentative detection of a weak absorption feature near 3050 cm^{-1} (3.28 μm) in the spectra of several Galactic center sources. If real, these features would most likely be due to C—H stretching vibrations of aromatic materials in the diffuse dust. If confirmed, this identification implies that on the order of 5% of the carbon in the diffuse ISM is tied up in aromatic materials.

These studies demonstrate the utility of comparing high-quality astronomical infrared spectra with the spectra of laboratory standards and analog materials. Future spectral comparisons of the type presented here should ultimately help unravel the organic chemical complexity of the ISM and may also help us determine whether the organic compounds in the primitive solar system bodies originated in the ISM, resulted from subsequent processing, or are the result of the combination of these effects. The data presented here provide an important step in that direction.

We thank the telescope operators at the NASA IRTF and the support staff of MKO. This work benefitted from discussions with several colleagues, especially Max Bernstein, Sherwood Chang, Dale Cruikshank, Peter Jenniskens, and Carl Sagan. The meteoritic data were kindly provided by W. G. Golden and the QCC data were kindly provided by Akira Sakata. We also thank Rose Grymes and Linda Jahnke in the Life Sciences Division at NASA-Ames for providing the laboratory sample of E-coli analyzed by Scott Sandford. We thank an anonymous referee for thoughtful comments and the extremely timely manner of his/her review of this manuscript. This work was partially supported by NASA grants 185-52-12-09 and 199-52-12-04 (Exobiology), 188-44-21-04 (Astrophysics), and 452-33-93-03 (Origins of Solar Systems).

REFERENCES

Abbott, D. C., & Conti, P. S. 1987, ARA&A, 25, 113
Adamson, A. J., Whittet, D. C. B., & Duley, W. W. 1990, MNRAS, 243, 400
Allamandola, L. J. 1991, in Proc. Internat. School of Physics "Enrico Fermi" Course III: Solid State Astrophysics, ed. E. Bussoletti & G. Strazzula (Amsterdam: North Holland), 1
Allamandola, L. J., & Sanford, S. A. 1988, in Dust in the Universe, ed. M. E. Bailey & D. A. Williams (Cambridge: Cambridge Univ. Press), 229
Allamandola, L. J., Sandford, S. A., & Valero, G. J. 1988, Icarus, 76, 225
Allamandola, L. J., Tielens, A. G. G. M., & Barker, J. R. 1985, ApJ, 290, L25
———. 1989, ApJS, 71, 733

Allen, C. W. 1973, Astrophysical Quantities (London: Athlone)
Amari, S., Lewis, R. S., & Anders E. 1994, Geochim. Cosmochim. Acta, 58, 459
Anders, E., & Zinner, E. 1993, Meteoritics, 28, 490
Baratta, G. A., & Strazzulla, G. 1990, A&A, 240, 429
Basile, B. P., Middleditch, B. S., & Oro, J. 1984, Org. Geochim., 5, 211
Becklin, E. E., & Neugebauer, G. 1975, ApJ, 200, L71
Becklin, E. E., Matthews, K., Neugebauer, G., & Willner, S. P. 1978a, ApJ, 219, 121
———. 1978b, ApJ, 220, 831
Bernstein, M. P., Sandford, S. A., Allamandola, L. J., & Chang, S. 1994a, J. Am. Chem. Soc., submitted
———. 1994b, in preparation
Bohlin, R. C., Savage, B. D., & Drake, J. F. 1978, ApJ, 224, 132
Borghesi, A. Bussoletti, E., & Colangeli, L. 1987, 314, 422
Bridger, A., Wright, G., & Geballe, T. 1993, in Conference Abstract Volume of Infrared Astronomy with Arrays: The Next Generation (Los Angeles: UCLA Dept. of Astronomy)
Brooke, T. Y., Tokunaga, A. T., & Knacke, R. J. 1991, AJ, 101, 268
Butchart, I., McFadzean, A. D., Whittet, D., Geballe, T. R., & Greenberg, J. M. 1986, A&A, 154, L5
Chyba, C., & Sagan, C. 1987, Nature, 329, 208
———. 1988, Nature, 332, 592
Cohen, M., Tielens, A. G. G. M., & Bregman, J. D. 1989, ApJ, 344, L13
Cohen, M., & Vogel, S. N. 1978, MNRAS, 185, 47
Cronin, J. R., & Chang, S. 1994, in Chemistry of Life's Origins, ed. J. M. Greenberg & V. Pirronella (Dordrecht: Kluwer), in press
Cronin, J. R., & Pizzarello, S. 1990, Geochim. Cosmochim. Acta, 54, 2859
Cruikshank, D. P., & Brown, R. H. 1987, Science, 238, 183
d'Hendecourt, L. B., & Allamandola, L. J. 1986, A&AS, 64, 453
d'Hendecourt, L. B., Allamandola, L. J., & Greenberg, J. M. 1985, A&A, 152, 130
DePoy, D. L., & Sharp, N. A. 1991, AJ, 101, 1324
De Vries, M. S., Reihs, K., Wendt, H. R., Golden, W. G., Hunziker, H., Flemming, R., Peterson, E., & Chang, S. 1993, Geochim. Cosmochim. Acta, 57, 933
Ehrenfreund, P., Robert, F., d'Hendecourt, L., & Behar, F. 1991, A&A, 252, 712
Gezari, D. Y. 1992, in The Center, Bulge, and Disk of the Milky Way, ed. L. Blitz (Dordrecht: Kluwer), 23
Greenberg, J. M. 1978, in Cosmic Dust, ed. J. A. M. McDonnell (New York: John Wiley), 187
Hayatsu, R., & Anders, E. 1981, Topics of Current Chemistry, 99, 1
Henry, J. P., DePoy, D. L., & Becklin, E. E. 1984, ApJ, 285, L27
Hoyle, F., Wickramasinghe, N. C., Al-Mufti, S., Olavesen, A. H., & Wickramasinghe, D. T. 1982, A&SS, 83, 405
Hudkins, D. M., Sandford, S. A., Allamandola, L. J., & Tielens A. G. G. M. 1993, ApJS, 86, 713
Humphreys, R. M. 1978, ApJS, 38, 309
Jones, A. P., Duley, W. W., & Williams, D. A. 1987, MNRAS, 229, 213
Kerridge, J. F., Chang, S., & Shipp, R. 1983, Geochim. Cosmochim. Acta, 51, 2527
Khare, B. N., Thompson, W. R., Cheng, L., Chyba, C., Sagan, C., Arakawa, E. T., Meisse, C., & Tuminello, P. S. 1993, Icarus, 103, 290
Krishnamurthy, R. V., Epstein, S., Cronin, J. R., Pizzarello, S., & Yuen, G. U. 1992, Geochim. Cosmochim. Acta, 56, 4045
Lebofsky, M. J., Rieke, G. H., & Tokunaga, A. T. 1982, ApJ, 263, 736
Lee, W., & Wdowiak, T. J. 1993, ApJ, 417, L49
Leger, A., & Puget, J. L. 1984, A&A, 137, L5
Lequeux, J., & Jourdain de Muizon, M. 1990, A&A, 240, L19
Lewis, R. S., Amari, S., & Anders, E. 1994, Geochim. Cosmochim. Acta, 58, 471
McFadzean, A. D., Whittet, D. C. B., Longmore, A. J., Bode, M. F., & Adamson, A. J. 1989, MNRAS, 241, 873
Ming, T., & Anders, E. 1988, Geochim. Cosmochim. Acta, 52, 1245
Mueller, B., Tholen, D., Hartmann, W., & Cruikshank, D. 1992, Icarus, 97, 150
Mullie, F., & Reisse, J. 1987, Topics Current Chem., 139, 83
Nugis, T. 1982, in Wolf-Rayet Stars: Observations, Physics, Evolution, ed. C. W. H. de Loore & A. J. Willis (Dordrecht: Reidel), 131
Ogmen, M., & Duley, W. W. 1988, ApJ, 334, L117
Pendleton, Y. J. 1993, PASP, 41, 171
———. 1994, PASP, 58, 255
Pendleton, Y. J., & Cruikshank, D. C. 1994, Sky & Telescope, 87, 36
Roche, P. F., & Aitken, D. K. 1984, MNRAS, 208, 481
———. 1985, MNRAS, 215, 425
Rieke, G. H., Rieke, M. J., & Paul, A. E. 1989, ApJ, 336, 752
Sakata, A., & Wada, S. 1989, in IAU Symp. 135, Interstellar Dust, ed. L. J. Allamandola & A. G. G. M. Tielens (Dordrecht: Kluwer), 191
Sakata, A., Wada, S., Onaka, T., & Tokunaga, A. T. 1987, ApJ, 320, L63
Sandford, S. A. 1984, Icarus, 60, 115
Sandford, S. A., Allamandola, L. A., Tielens A. G. G. M., Sellgren, K., Tapia, M., & Pendleton, Y. 1991, ApJ, 371, 607
Sandford, S. A., Pendleton, Y. J., & Allamandola, L. J. 1994, ApJ, submitted
Schulte, D. H. 1958, ApJ, 128, 41
Schutte, W. 1988, Ph.D. thesis, Univ. of Leiden
Sellgren, K., Hall, D. N. B., Kleinmann, S. G., & Scoville, N. Z. 1987, ApJ, 317, 881
Sellgren, K., Smith, R., & Brooke, T. Y. 1994, ApJ, 433, 179
Sneden, C., Gehrz, R. D., Hackwell, J. A., York, D. G., & Snow, T. P. 1978, ApJ, 223, 168
Tielens, A. G. G. M., & Allamandola, L. J. 1987, in Physical Processes in Interstellar Clouds, ed. G. E. Morfill & M. Scholer (Dordrecht: Reidel), 333
Tokunaga, A. T., ed. 1986, IRTF Photometry Manual (Honolulu: Univ. Hawaii)
Tokunaga, A. T., & Brooke, T. Y. 1990, Icarus, 86, 208
Tokunaga, A. T., Smith, R. G., & Irwin, E. 1987, in Infrared Astronomy with Arrays, ed. C. G. Wynn-Williams, E. E. Becklin, & L. H. Good (Honolulu: Univ. Hawaii), 367
Tollestrup, E. V., Capps, R. W., & Becklin, E. E. 1989, AJ, 98, 204
Torres, A. V. 1988, ApJ, 325, 759
Wade, R., Geballe, T. R., Krisciunas, K., Gatley, I., & Bird, M. C. 1987, ApJ, 320, 570
Wickramasinghe, D. T., & Allen, D. A. 1980, Nature, 287, 518
White, R. L., & Becker, R. H. 1983, ApJ, 272, L19
Williams, P. M., van der Hucht, K. A., & Thé, P. S. 1987, A&A, 182, 91
Willis, A. J. 1982, In Wolf-Rayet Stars: Observations, Physics, Evolution, ed. C. W. H. de Loore & A. J. Willis (Dordrecht: Reidel), 87
Witteborn, F. C., Sandford, S. A., Bregman, J. D., Allamandola, L. J., Cohen, M., Wooden, D. H., & Graps, A. L. 1989, ApJ, 341, 270
Wright, G., Bridger, A., Geballe, T., & Pendleton, Y. J. 1994, in preparation